JOURNAL OF INTERFERON & CYTOKINE RESEARCH
Volume 30, Number 7, 2010

DOI: 10.1089/jir.2009.0105

Early Differential Expression of Oncostatin M in Obstructive Nephropathy

Wafa M. Elbjeirami,[1] Luan D. Truong,[2] Ahmad Tawil,[3] Wansheng Wang,[4] Sara Dawson,[3] Hui Y. Lan,[5] Ping Zhang,[4] Gabriela E. Garcia,[4] and C. Wayne Smith[3]

Interstitial fibrosis plays a major role in progression of renal diseases. Oncostatin M (OSM) is a cytokine that regulates cell survival, differentiation, and proliferation. Renal tissue from patients with chronic obstructive nephropathy was examined for OSM expression. The elevated levels in diseased human kidneys suggested possible correlation between OSM level and kidney tissue fibrosis. Indeed, unilateral ureteral obstruction (UUO), a model of renal fibrosis, increased OSM and OSM receptor (OSM-R) expression in a time-dependent manner within hours following UUO. *In vitro*, OSM overexpression in tubular epithelial cells (TECs) resulted in epithelial-myofibroblast transdifferentiation. cDNA microarray technology identified up-regulated expression of immune modulators in obstructed compared with sham-operated kidneys. *In vitro*, OSM treatment up-regulated CC chemokine ligand CCL7, and CXC chemokine ligand (CXCL)-14 mRNA in kidney fibroblasts. *In vivo*, treatment of UUO mice with neutralizing anti-OSM antibody decreased renal chemokines expression. In conclusion, OSM is up-regulated in kidney tissue early after urinary obstruction. Therefore, OSM might play an important role in initiation of renal fibrogenesis, possibly by inducing myofibroblast transdifferentiation of TECs as well as leukocyte infiltration. This process may, in turn, contribute in part to progression of obstructive nephropathy and makes OSM a promising therapeutic target in renal fibrosis.

Introduction

Tubulointerstitial fibrosis is presently considered a final common pathway of progressive kidney disease leading to end-stage renal disease. It is characterized by loss of renal tubules and accumulation of myofibroblasts and extracellular matrix (ECM) proteins (Lan 2003). Myofibroblasts are rare in the normal kidney; however, they appear in markedly increased numbers in the fibrotic kidney. The origin of myofibroblasts within the diseased kidney remains poorly understood. Emerging evidence suggests that during renal injury, tubular epithelial cells (TECs) transdifferentiate into myofibroblasts in a process known as epithelial-myofibroblast transdifferentiation (EMT) (Hay and Zuk 1995; Ng and others 1998). EMT is a physiological process associated with fibrogenesis related to a number of adult organs including the liver, the thyroid, and the mammary glands (Strutz and Müller 2000). Transdifferentiation in TECs has been demonstrated *in vivo*. In kidney with urinary obstruction, TECs exhibited features of EMT, as well as increased transforming growth factor β1 (TGF-β1) expression (Dauthville and others 1998; Yang and Liu 2001).

The mechanism(s) regulating renal tubular EMT remains largely unknown. A number of studies have analyzed the possible effects of cytokines and matrix components on EMT (Hay and Zuk 1995; Zeisberg and others 1999; Healy and others 1999). *In vitro* studies previously demonstrated that tubular EMT can be induced by profibrotic cytokines such as TGF-β, fibroblast growth factor-2, epithelial growth factor, and IL-1β (Okada and others 1997; Fan and others 1999; Stahl and Felsen 2001; Manotham and others 2004). These studies demonstrate clearly that the differentiation state of the TEC is dependent on the surrounding ECM and on

[1]Department of Pathology and Laboratory Medicine, King Hussein Cancer Center, Amman, Jordan.
[2]Department of Pathology, Methodist Hospital, Houston, Texas.
[3]Section of Leukocyte Biology, Children's Nutritional Research Center and [4]The Renal Section, Baylor College of Medicine, Houston, Texas.
[5]Department of Medicine, University of Hong Kong, China.

cytokines secreted by adjacent cells. However, those studies were hypothesis-driven, with each factor being investigated alone and generating downstream events that ultimately contributed to renal fibrosis or its reversal.

Oncostatin M (OSM) is a multifunctional member of the interleukin-6 cytokine family and is produced from activated T- and monocytic cell types (Tanaka and Miyajima 2003). OSM is a growth and differentiation factor that participates in the regulation of neurogenesis, osteogenesis, and hematopoiesis. Nightingale and others (2004) have demonstrated that human proximal TECs undergo EMT in response to OSM produced by activated peripheral blood mononuclear cell (aPBMC-CM), showing acquisition of a fibroblastoid morphology, increased fibronectin-EDA (EDA) expression, loss of junctional E-cadherin localization, and cytokeratin 19 (CK19) expression. The group proposed that OSM is likely produced by inflammatory cell infiltrates that contribute to tubulointerstitial fibrosis.

We investigated whether OSM might be associated with renal fibrosis *in vivo* by examining the expression of this gene in kidney with obstructive nephropathy, a condition characterized by tubular atrophy, interstitial fibrosis, and fibroblast proliferation. We report here for the first time that OSM expression is highly elevated in kidneys from patients with urinary obstruction. Furthermore, we showed that unilateral ureteral obstruction (UUO), a well-characterized experimental model of obstructive nephropathy, is associated with *de novo* expression of OSM and its receptor (R) in the nephron very early following UUO. Thus, OSM expression in renal obstruction may play a role in driving tubulointerstitial fibrosis via EMT mechanism.

Materials and Methods

Human renal tissue

Renal tissue from 5 patients with urinary obstruction of variable causes was included in this study. "Normal" kidney tissue from 4 nephrectomy specimens with localized renal tumors was used for control. The human tissue was used following the guidelines of the Ethics Committee of Baylor College of Medicine.

Obstructive nephropathy model

Progressive obstructive nephropathy was induced in wild-type male mice (15–20 g body weight), or male Sprague-Dawley rats (200–225 g body weight) by left ureter ligation as described previously (UUO) (Fukuda and others 2001; Lan and others 2003). Groups of 3 animals were killed at designated times after the operation. All experimental procedures were approved by the Animal Experimental Committee at Baylor College of Medicine.

Injection of anti-oncostatin antibody

Groups of 5 normal male C57/BL6 mice (20–25 g) were given intraperitoneal (i.p.) injections of anti-oncostatin polyclonal antibody (AF-495-NA; R&D Systems, Minneapolis, MN) or normal goat IgG (R&D Systems) at 1 mg/kg 2 h prior to surgery. After the animals underwent UUO as described earlier, they received the same antibody treatment 1 h after surgery. Kidneys were harvested at 6 h post-UUO for real-time PCR analysis of chemokine expression.

Cell culture and transfection

The entire coding region of rat OSM cDNA was generated by RT-PCR with a set of primers, the sequence being forward 5′-ACAATGCGGGCTCAGCCTCCA, and reverse 5′-AATTACCGGGGCACCAGGGA. Rat OSM cDNA was then cloned into a retroviral expression vector (PLE-GFP-N1; Clontech, Mountain View, CA). Retrovirus was produced by transient transfection of the amphotropic Phoenix packaging cell line (protocol detailed at www.stanford.edu/group/nolan). Rat renal TECs (NRK52E) were plated at 7,500 cell/cm^2 and supplemented with the viral supernatant at 1 mL/10 cm^2. Retroviral transduction with enhanced green fluorescence protein (eGFP) was used for mock transfections as a control.

OSM stimulation of mouse renal fibroblasts

Mouse renal fibroblasts were isolated from C57/BL6 wild-type mouse kidneys. Kidneys were removed using sterile instruments, minced, digested with Liberase Blendzyme 3 (Roche diagnostics, Indianapolis, IN) in Dulbecco's modified Eagle's medium (DMEM) at final concentration of 0.3 mg/mL and then incubated at 37°C in a humidified atmosphere of 5% CO_2 in air for 2–4 h. Digested tissue were washed with DMEM containing 10% fetal calf serum (FCS) at 5 min 1,000 rpm and finally resuspended in this medium. Cells were then incubated at 37°C in a humidified atmosphere of 5% CO_2 in air. After 4 h, unattached cells were removed by washing, and fresh medium was added and incubated at 37°C until fibroblast confluence. The MKF were subcultured in T-25 flasks to near confluence in serum-containing medium, followed by 24 h of incubation in serum-free conditions before stimulation. For stimulation, cells were either left untreated or treated with 1, 10, 100, or 200 ng/mL recombinant OSM (R&D Systems, Minneapolis, MN) in DMEM media supplemented with 0.5% BCS for 24 h. Following a 24-h stimulation with OSM, chemokine CXCL1, CXCL2, CXCL5, CXCL14, CCL2, CCL4, CCL5, and CXCL7 mRNA expressions were measured by real-time RT-PCR and normalized to controls as described in the following section.

Real-time PCR

After total cells and kidney RNA were isolated using TRIzol® (Invitrogen, Carlsbad, CA), it was reversely transcribed into complimentary DNA (cDNA) as described elsewhere (Ng and others 1999). Complementary RNA was amplified by real-time quantitative polymerase chain reaction (PCR) (TaqMan®, ABI Prism 7500 Sequence Detection System, Foster City, CA) using fluorogenic probes. GAPDH or 18S were used as an internal standard in the comparative threshold cycle method using ($2^{-\Delta Ct}$). Final values were determined as the ratio for the gene of interest to GAPDH or 18S and expressed as the means ± SEM. Samples were measured in triplicates.

RNase protection assay

RPA was performed as previously described (Feng and others 2000). In brief, 5 µg of total RNA for each sample prepared from tissue were used in RNase protection assay. Riboprobe specific for rat OSM was prepared (nucleotides

117–520 as defined in GeneBank sequence accession number NM_001006961). RNase protection assay was performed using a kit (Torrey Pines Biologicals, Houston, TX) according to the manufacturer's protocols with corresponding probes labeled with [^{32}P] UTP.

Immunohistochemistry

Four-micrometer tissue sections were deparaffinized in xylene and rehydrated in graded alcohol series. The sections were heated in a target retrieval solution (pH 6.0; Dako, Carpinteria, CA) for 10 min in a high voltage microwave to facilitate antigen retrieval. Immunohistochemical staining was performed using an avidin–biotin–peroxidase complex technique (Vector Laboratories, Burlingame, CA). The sections were incubated with the following primary antibodies overnight at 4°C: polyclonal rabbit anti-human OSM antibody (1:1,500; Santa Cruz Biotechnology, Santa Cruz, CA), goat anti-mouse OSM antibody (1:100; Santa Cruz Biotechnology), or rabbit anti-mouse OSM antibody (1:100; Santa Cruz Biotechnology). As a negative control, the primary antibody was replaced by non-immune serum from the same species. Slides were developed with diaminobenzidine tetrahydrochloride (DAB; Sigma, St. Louis, MO) and counterstained with hematoxylin.

Immunofluorescence

Confluent-transfected NRK52E cells grown on glass coverslips were fixed with 1% formaldehyde (Tousimis, MD), permeabilized with 0.1% Triton X-100, and blocked for 30 min with goat serum. Next, cells were incubated with anti-E-Cadherin (Transduction Laboratories, Lexington, KY), washed 3 times, and incubated with anti-mouse directly labeled with AlexaFluor-568 (Invitrogen, Carlsbad, CA). Finally, the slides were mounted with Airvol and visualized using a Deltavision Deconvolution microscope (Applied Precision, Issaqua, Washington).

Western blot analysis

Cells and tissues were lysed in RIPA buffer (Sigma-Aldrich, St. Louis, MO) with complete protease inhibitor (Roche Biochemicals, Indianapolis, IN). The 20 µg of protein was separated by SDS-PAGE, transferred to nitrocellulose membranes, and blocked in 5% skim milk in TBS-T (TBS, 0.05% Tween-20) overnight. The primary antibody and peroxidase-conjugated secondary antibody (1:5,000) incubations were carried out for 3 and 1 h, respectively. The signals were visualized by an enhanced chemiluminescence (ECL) system (GE Life Science, Piscataway, NJ). The primary antibodies used were as follows: goat anti-OSM (1:100; Santa Cruz Biotechnology, Santa Cruz, CA), rabbit anti-OSM receptor (1 µg/mL; R&D Systems, Minneapolis, MN), mouse anti-α-SMA (1:1,000; Dako), mouse anti-E-cadherin (1:2,000; Transduction Laboratories, Lexington, KY), and rabbit anti-actin (1:300; sc-10731, Santa Cruz Biotechnology).

Measurement of transcellular electrical impedance

Electrode fabrication and the design of electric cell–substrate impedance sensor (ECIS) have been reported previously (Lo and others 1993). The electrical resistance of NRK monolayers was measured with the electrical cell impedance sensor technique. In this system (Applied Biophysics, Troy, NY), the cells are cultured on a small gold electrode (10^{-4} cm^2) in DMEM supplemented with 10% FBS. Cell–cell adhesion was recorded as an increase in the electrical resistance. Electrical resistance increased immediately after the cells attached to and covered the electrodes, and the resistance achieved a steady state when the cells became confluent. Thus, the data were plotted after the electrical resistance achieved a steady state.

Microarray analysis

UUO was induced in wild-type male mice as described earlier (Fukuda and others 2001; Lan and others 2003). Sham-operated and UUO kidney tissue was collected 3 h after UUO for homogenization in TRIzol® followed by RNA extraction according to the manufacturer's instructions. All RNA samples were treated with 5 U RNase-free DNase I (Qiagen, Valencia, CA) to eliminate any contaminating DNA, and then purified using a Qiagen RNeasy Mini kit according to the RNA cleanup protocol. RNA quality was assessed using the Agilent 2100 bioanalyzer (Agilent Technologies, Palo Alto, CA).

Gene expression analysis was performed at Baylor College of Medicine Microarray Core Facility. In brief, total RNA was biotinylated and hybridized to GeneChip® Mouse Genome 430 2.0 Array (Affymetrix, Santa Clara, CA) according to manufacturer's instructions (www.affymetrix.com/pdf/expression_manual.pdf/). For statistical analysis, we used 2-way analysis of variance (ANOVA, assuming equal variance). We used a P value cutoff of 0.005 and a gene expression fold-difference threshold of 1.2 (for either up-regulation or down-regulation) for all our analyses. Gene expression was defined "positive" when detected by microarrays in all groups tested. A total of 3 pairs (sham-operated and UUO) of kidneys were included for microarray analysis. All samples were run in duplicate. The Gene Ontology overrepresentation analyses were performed with the help of the software application DAVID, http://apps1.niaid.nih.gov/david (Hosack).

Statistical analysis

Data are expressed as the mean ± SEM. Statistical differences were analyzed using analysis of variance and pairwise multiple comparisons using Tukey's test, and P values <0.05 were considered to indicate statistical significance.

Results

OSM expression in human obstructed kidneys

Oncostatin M expression was determined in human kidney tissue with obstructive nephropathy and in control normal kidney tissue. Real-time PCR analysis revealed that OSM mRNA was elevated by 6-fold in kidney samples collected from patients with obstructive nephropathy due to stones or carcinoma (Fig. 1A). Similarly, Western blot analysis confirmed increased OSM protein expression in these obstructed kidneys (Fig. 1B) as compared with normal kidney tissue. Furthermore, immunostaining showed marked OSM expression in TECs, glomeruli, inflammatory infiltrates, as well as the endothelium in obstructed kidney

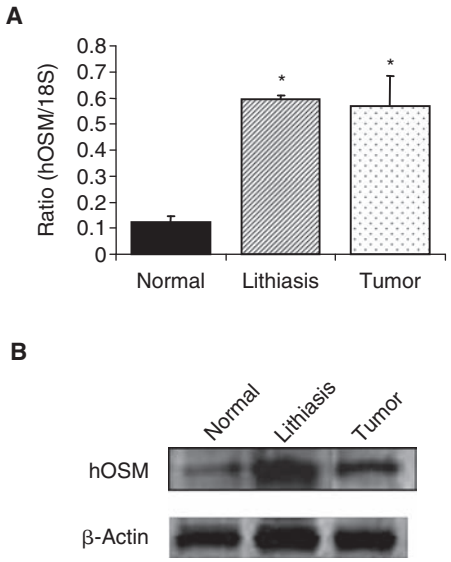

FIG. 1. Oncostatin M (OSM) expression levels in renal tissue from patients with chronic obstructive nephropathy. (**A**) Real-time RT-PCR analysis shows substantially higher OSM mRNA in obstructed kidneys with tubulointerstitial fibrosis due to lithiasis or tumor, compared with normal control kidney. *$P < 0.01$ compared with normal kidney. (**B**) Western blot of representatives of the same tissue samples confirms the increased expression of OSM.

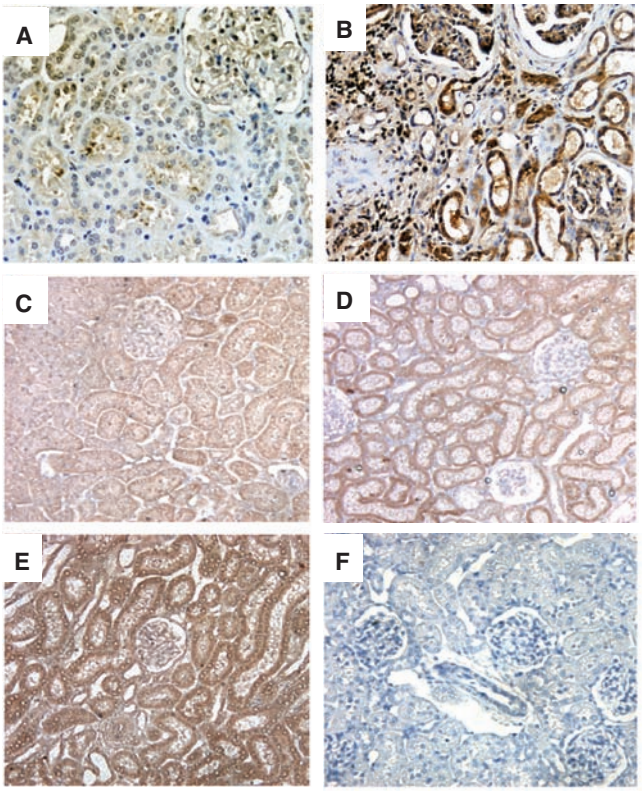

FIG. 2. Oncostatin M (OSM) expression in renal tissue. (**A** and **B**) Immunohistochemistry of OSM in human kidney. Immunostain shows strong expression of OSM in atrophic tubular cells, glomerular cells, and interstitial inflammatory cells in a representative kidney with obstructive nephropathy (**B**). Only weak, focal expression of OSM is noted in a representative normal kidney (**A**). Original magnification: 200×. (**C**–**F**) Immunohistochemistry of OSM in control normal kidneys of rats (**C**), and obstructed kidneys at 12 h (**D**) and 24 h (**E**) after UUO. Increased expression of OSM is evident in renal tubular cells of the obstructed kidneys. Control IgG shows no staining for OSM (**F**). The results are representative of kidneys derived from 3 different animals. Original magnification: 200×.

(Fig. 2B), whereas insignificant expression was noted in normal kidney sections (Fig. 2A). Overall, these results suggested a correlation between renal OSM expression and urinary obstruction-mediated chronic tubulointerstitial fibrosis in human. Thus, we decided to explore OSM expression in UUO, a well-characterized hydronephrosis model exhibiting interstitial inflammatory cell infiltration and tubular dilatation.

OSM and OSM-R expression in UUO

Progressive tubulointerstitial fibrosis of the kidney secondary to UUO was created in rat and mice to see whether OSM expression was associated with renal changes. RNase protection assay revealed increased OSM mRNA levels in the rat UUO kidneys compared with normal kidneys, as early as 3 h after obstruction, and persisting even at 24 h (Fig. 3A). Time-course analysis of OSM and OSM-R using real-time PCR revealed a 2- and 3-fold increase in OSM expression as early as 3 and 6 h after obstruction in the mouse and rat kidney, respectively (Fig. 3B). By 24 h, a marked increase was evident in the obstructed kidney of both animal models, with markedly elevated levels seen by 1 week in the mouse UUO kidney (8-fold). Similar results were also obtained when we examined OSM-R levels in obstructed mouse and rat kidneys, but a higher magnitude

FIG. 3. Unilateral ureteral obstruction (UUO) induces the expression of Oncostatin M (OSM) and OSM receptor mRNA. (**A**) Time course of OSM mRNA expression in left obstructed rat kidneys, and control kidneys (control) 1, 3, 6, 12, and 24 h after UUO. Ribonuclease protection assays (RPA) were performed with total RNA prepared from an entire kidney to quantitate mRNA levels for *OSM* and control ribosomal protein L32 (*rPL32*). Representative gel segments from 2 (a, b) obstructed and 2 control kidneys per time point showed a progressive up-regulation of mRNA encoding for OSM during the course of UUO as compared with control kidney. The sizes of protected fragments for both mRNA species are indicated with arrows. (*Below*) Semiquantitative data using densitometric analysis of OSM relative to L32. *$P < 0.05$. (**B**) Renal expression of OSM and OSM receptor mRNA was determined by real-time RT-PCR from total renal isolates at designated time points after unilateral ureteral obstruction (UUO) in the mouse or rat. Data are presented as the fold increase of OSM mRNA expression in obstructed kidneys (UUO) normalized to non-ligated control kidneys (time 0). Each bar represents the mean ± SEM for a group of 3 animals. *$P < 0.01$, **$P < 0.05$ versus normal controls.

of increase for the receptor was seen at some time points compared with OSM expression (Fig. 3B). For example, obstructed mouse kidney exhibited a 2-fold increase in OSM expression, but a 7-fold increase in OSM-R at 24 h after UUO. Similarly, the UUO rat kidneys exhibited a 3-fold increase in OSM expression and a 6-fold increase in OSM-R at 12 h

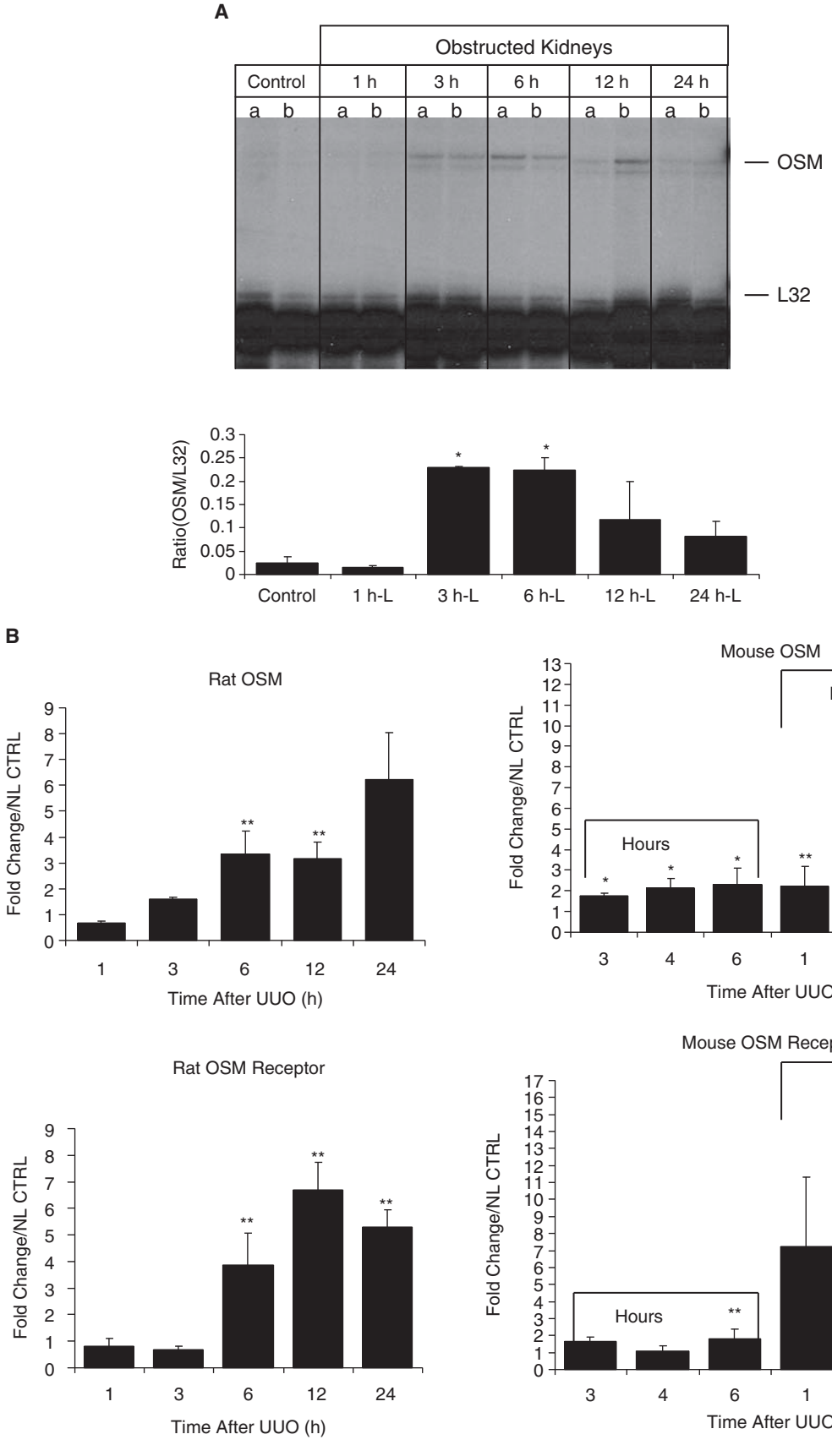

after UUO. OSM and OSM-R levels of the contralateral unobstructed kidney and of normal control kidney were similar by real-time PCR at all time points following UUO (data not shown). Furthermore, Western analysis verified increased OSM protein and its receptor in the obstructed samples at 6 and 24 h following UUO based on the intensity of the bands (Fig. 4A).

Localization of OSM protein by immunohistochemistry

To determine sites of OSM protein expression, we performed immunolabeling with anti-OSM antibody. Immunohistochemical staining showed the nephron segments were positive for OSM protein in both control (Fig. 2C) and obstructed rat kidneys at 12 and 24 h after UUO (Fig. 2D and 2E, respectively). However, there was a more prominent staining of TECs in UUO kidneys. A control experiment with a non-immune serum did not show any tissue staining (Fig. 2F).

Expression of EMT markers early after UUO

Because OSM has been implicated to promote EMT *in vitro* (Nightingale and others 2004), we examined the possibility that α-smooth muscle actin (α-SMA) and collagen type I, 2 EMT markers, may exhibit differential expression early in UUO correlating with changes in OSM levels. Relative real-time PCR demonstrated no differences in α-SMA, and collagen type I mRNA levels during the first 24 h following UUO in rats (Fig. 4B). Western blot analysis also revealed no increase in the EMT markers during the first day following renal obstruction (data not shown).

OSM overexpression in cultured renal tubular cells

To address whether OSM can cause EMT in rodent TECs, NRK52E cells were retrovirally transduced to overexpress OSM cDNA. GFP control transduction revealed at least 95% of cells were positive for gene overexpression (Fig. 5C). OSM overexpression was confirmed by Western analysis revealing higher OSM protein level in OSM-transfected cells as compared with GFP-transfected cells (Fig. 5E). The control GFP-transfected cells maintained a typical cobblestone epithelial morphology (Fig. 5A). However, the OSM-transfected cells exhibited focal areas with mesenchymal features as well as loss of contact inhibition (Fig. 5B), which was further demonstrated by immunofluorescence for E-cadherin showing higher levels in GFP-transfected cells (Fig. 5C) as compared with OSM-expressing cells (Fig. 5D). EMT markers were next analyzed by Western blotting. While α-SMA level (marker for myofibroblastic phenotype) has dramatically increased in OSM-transfected NRK52E cells, the E-cadherin level (marker for epithelial phenotype) markedly decreased in OSM-transduced cells (Fig. 5E).

Effect of OSM on the barrier function of the NRK cells

Exposure to OSM resulted in suppression of kidney E-cadherin (major cell–cell adhesion protein) levels as demonstrated earlier. Consequently, we examined the effect of OSM on cell–cell adhesion of TECs. The attachment of OSM-transfected and GFP-transfected TECs to microelectrodes was examined. Transcellular resistance was recorded after the cells reached full confluency for 29 continuous hours. When GFP-transfected cells were seeded on the surface of electrodes, cell attachment and spreading resulted in an increase of the resistance (Fig. 5F). In contrast, OSM overexpression in TECs resulted in lower resistance recordings; thus supporting the notion that OSM affects tubular epithelial cell–cell adhesion and implying observed spontaneous fluctuations in cell resistance could be attributed to changes in adhesive interactions.

Changes in gene expression early following UUO

We performed cDNA microarray analysis to elucidate dynamic changes in gene expression following UUO. Because we observed differential OSM expression as early as 3 h in UUO animals, we chose this time point to analyze any alterations of gene expression following obstruction. We used Affymetrix mouse GeneChip 430 2.0 microarray to compare and select genes as described in the Materials and Methods section. A total of 238 genes passed the selection criteria. Murine kidneys subjected to UUO for 3 h ($N = 3$)

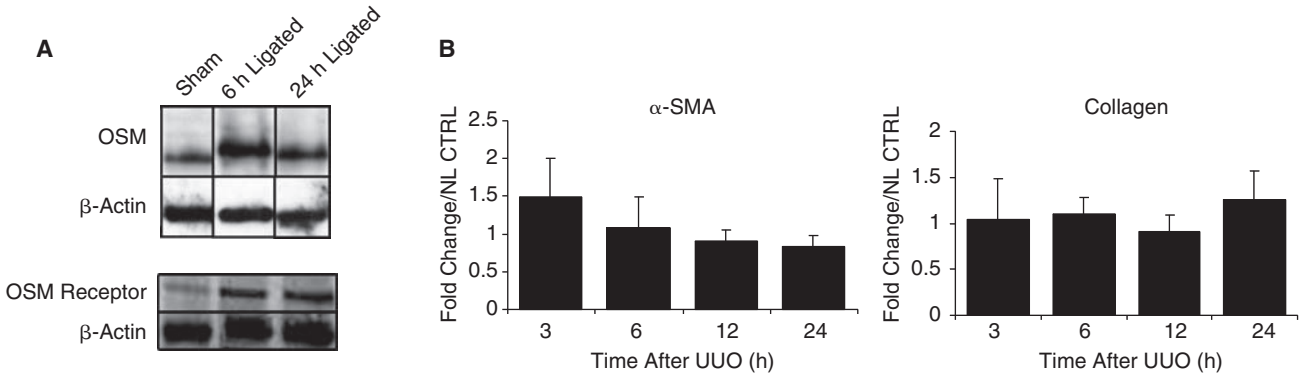

FIG. 4. (**A**) Oncostatin M (OSM) and OSM receptor protein expression is up-regulated by unilateral ureteral obstruction (UUO). Expression of OSM and OSM receptor in UUO rat kidneys and in normal control kidneys at 6 and 24 h after obstruction by Western blot analysis. (**B**) Real-time PCR analysis of α-SMA and collagen I EMT markers following UUO in rats. No difference in α-SMA and Col I mRNA levels is observed in the first 24 h following UUO.

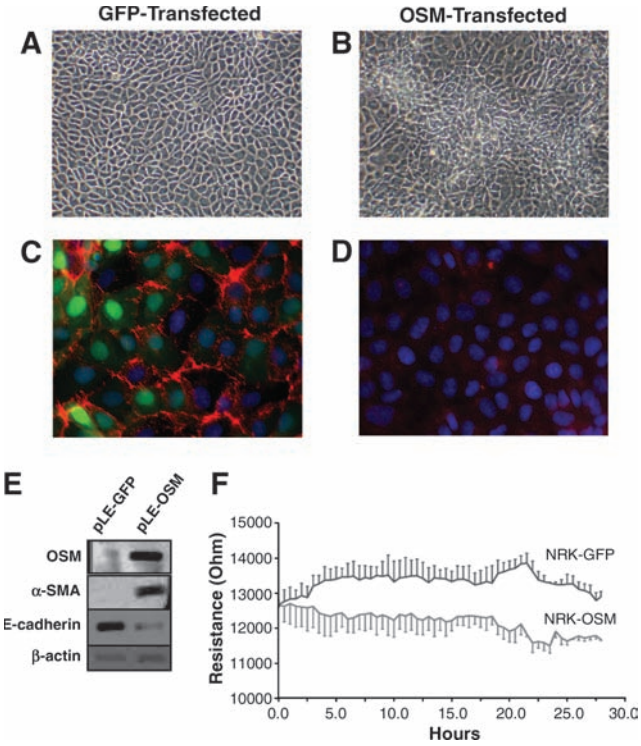

FIG. 5 OSM overexpression in tubular epithelial cells induces TEC-myofibroblast transdifferentiation. (**A**) Control GFP-transfected cells display typical epithelial morphology, including cuboidal cells forming regular monolayers. In contrast, (**B**) OSM-transfected cells show focal areas with mesynchymal features (center) including cells with spindled morphology forming layers, indicating a loss of contact inhibition (magnification of ×200). (**C**) Immunofluorescent staining shows a marked expression of E-cadherin (red), an epithelial marker, in control GFP-transfected cells (green demonstrates GFP transfection efficiency in GFP-expressing NRK52E cells), but E-cadherin staining is very low in OSM-transfected cells (**D**) (magnification of ×400). (**E**) Western blot analyses demonstrate that overexpression of OSM in NRK52E cells (lane 2) induces *de novo* expression of α-SMA, and a loss of E-cadherin compared to GFP-transfected cells (lane 1). (**F**) Real-time recordings of the electrical impedance as an indicator of cell adhesion. Rate of epithelial cell adhesion on microelectrode surface is decreased in OSM-expressing cells as compared to control GFP-transfected cells. All tracings are representative of three experiments.

were compared with their respective unobstructed contralateral kidneys as control ($N = 3$). Figure 6 shows a summary of selected genes we were interested in pursuing. An induction of transcripts was observed for genes encoding cytokines including OSM, which was up-regulated by 1- to 3-fold in UUO kidneys as compared with control nonoperated kidneys (Fig. 6). Other proinflammatory cytokines up-regulation was observed in interleukin-6 (IL-6) and leukemia inhibitory factor (LIF), a closely related member of OSM belonging to IL-6 family. Furthermore, there was a marked increase in TGF-β, a profibrotic mediator, as well as tumor necrosis factor (TNF-α). Many cytokine-stimulated adhesion molecules were up-regulated following obstruction compared with non-obstructed kidney counterparts. UUO also

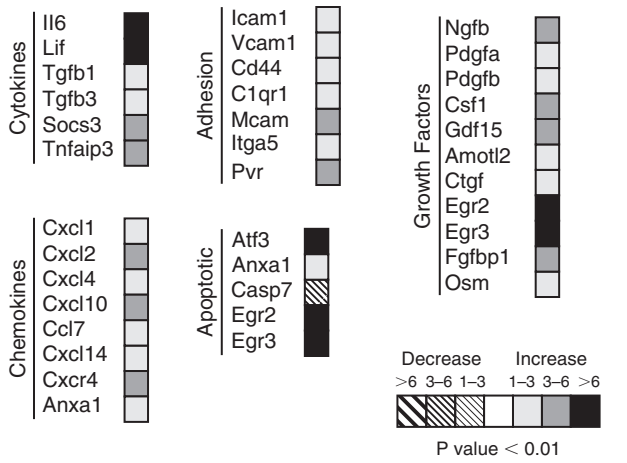

FIG. 6. Gene expression profiles at 3 h obtained from sham-operated and unilateral ureteral obstruction (UUO) murine kidneys.

induced the transcription of genes encoding growth factor proteins and proinflammatory chemokines, with CXCL2 being the most prominent chemokine in obstructed kidneys (>6-fold change over control).

OSM-mediated induction of chemokines

Because our microarray data showed a significant up-regulation of chemokine production, we investigated which chemokines specifically respond to OSM treatment of kidney epithelial cells *in vitro*. Results showed a dose-dependent increase with a peak of 15-fold for CXCL14 mRNA expression and 10-fold for CCL7 mRNA expression consistent with results obtained from microarray study described earlier (Fig. 7).

Effects of OSM neutralization early in UUO

Because local expression of chemokines mediates renal leukocyte recruitment, we investigated whether administration of a neutralizing antibody to OSM could affect local production of CC- and CXC-chemokines in obstructed kidneys. We performed real-time RT-PCR for CCL4, CCL7, CXCL1, CXCL2, and CXCL14 mRNA on total renal isolates from anti-OSM Ab and IgG control-treated mice at 6 h after UUO. Induction of renal fibrosis by UUO resulted in chemokine mRNA overexpression that was significantly reduced by the treatment with the neutralizing OSM antibody. At 6 h after UUO, control mice exhibited a mean 140-fold increase of CXCL1 mRNA, a mean 40-fold increase of CXCL2 mRNA, and a mean 4-fold increase of CXCL14 and CCL7 in the obstructed kidneys as compared with the non-obstructed kidneys of the same animal. Treatment with the neutralizing anti-OSM antibody led to a significant 85% reduction of renal CXCL1 mRNA expression as well as a significant 88% reduction of renal CXCL2 mRNA expression compared with mice treated with irrelevant IgG control. There was also a significant decrease in CCL7 and CXCL14 chemokine expression in anti-OSM-treated mice (Fig. 8). However, we did not observe any differences in CCL4 expression.

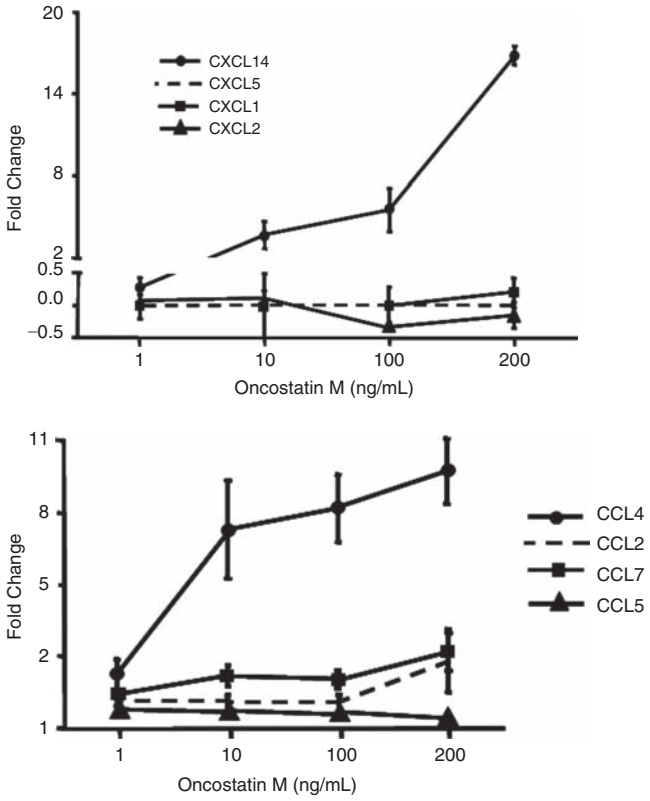

FIG. 7. Effect of Oncostatin M (OSM) treatment on chemokine expression in mouse kidney fibroblasts. Mouse kidney fibroblasts were stimulated with different concentrations of recombinant OSM for 24 h. Following OSM stimulation, the chemokines CCL7 and CXCL14 were both increased on the mRNA level.

Discussion

Emerging evidence suggests that during renal injury, TECs are capable of transdifferentiating into myofibroblasts in a process known as tubular EMT (Hay and Zuk 1995; Ng and others 1998). The proposed mechanisms that lead to EMT are diverse but center around changes in the ECM, cytokines, growth factors, adhesion molecules, and hypoxia (Okada and others 1997; Dauthville and others 1998; Fan and others 1999; Healy and others 1999; Zeisberg and others 1999; Stahl and Felsen 2001; Yang and Liu 2001; Lan 2003). Healy and others (1999) incubated human proximal TECs with supernatant from activated peripheral blood mononuclear cells and observed changes in phenotype to a fibroblast-like morphology. Moreover, this treatment resulted in a significant decrease in transepithelial resistance and in expression of the epithelial junctional proteins E-cadherin and occludin. Nightingale and others (2004) used cDNA microarray analysis to assess changes in gene expression to identify novel molecular mechanisms driving EMT. The group determined OSM to be a novel inducer of EMT and is likely produced by inflammatory cell infiltrates. In the present study, we demonstrated for the first time the following: (1) increased levels of OSM and OSM-R expression in human or rodent kidney with obstructive nephropathy in a time-dependent manner. (2) Specific depletion of OSM using neutralization antibody reduces specific chemokine production after UUO demonstrating that OSM plays a key role in the pathogenesis of renal fibrosis.

First, we demonstrated the correlation between OSM/OSM-R system with renal fibrosis. Analyses of kidney tissue from patients with chronic obstructive nephropathy at various stages of development indicated that OSM expression is highly up-regulated and therefore may play a role in promoting renal fibrosis via induction of EMT. EMT has been observed in renal biopsy tissues (Jinde and others 2001; Rastaldi and others 2002). Nadasdy and others (1994) reported that single cells or loosely organized small cell clusters still positive for epithelial markers could be found in the widened interstitium of human kidneys with end-stage renal disease, consistent with the notion of EMT. A study of human renal biopsies of different renal diseases demonstrated that the number of TECs with EMT features was correlated with the degree of interstitial damage, indicating that EMT participates in the fibrotic process in human kidneys (Rastaldi and others 2002). Using microarray studies performed on human renal transplant implantation biopsies, Luyckx and others (2009) demonstrated that OSM and OSM-R were progressively expressed in human biopsies spanning a spectrum of renal injury. Indeed, both OSM and its receptor expression levels correlated with severity of renal injury. In our study, patients with renal obstruction produced higher levels of OSM message (6-fold) compared with normal kidneys. Consistently, increased OSM protein predominantly in TECs suggests a role OSM could play in driving renal fibrosis. OSM as a profibrotic cytokine has been associated with various types of tissue fibrosis. Increased amounts of OSM mRNA or protein have been related to development of pulmonary fibrosis in patients with systemic sclerosis (Hasegawa and others 1999). Transgenic mice overexpressing OSM exhibited increased fibrosis surrounding their pancreas (Malik and others 1995). *In vitro*, OSM induces collagen production (Scaffidi and others 2002), regulates production of tissue inhibitor of metalloproteinase-1 and -3 (Gatsios and others 1996), and enhances the growth of fibroblasts (Scaffidi and others 2002).

We and other groups propose that OSM plays a role in driving renal fibrosis by inducing EMT; a process by which epithelial cells lose cell–cell attachment, polarity, and epithelial-specific markers, undergo cytoskeletal remodeling, and gain a mesenchymal phenotype. The emerging paradigm is that EMT plays a prominent role in fibrogenesis in adult tissues. Growth factors such TGF-β, epidermal growth factor (EGF), and fibroblast growth factor 2 (FGF2) can induce EMT of TECs (Okada and others 1997; Fan and others 1999; Stahl and Felsen 2001). TGF-β levels are increased in the lungs of patients with fibrotic pulmonary diseases. TGF-β also induces EMT of alveolar epithelial cells, and fibroblastic cells that express both epithelial and mesenchymal markers can be detected in human biopsies (Thiery and Sleeman 2006). Furthermore, significant evidence indicates TGF-β-induced EMT of lens epithelial cells may be an important event during cataract formation and injury-induced lens-capsule fibrosis (De Longh and others 2005). On the other hand, OSM as a promoter of EMT has been previously studied in the liver (Okaya and others 2005), osteoblasts (Malaval and others 2005), and neurons (Morikawa and others 2004). A previous study revealed that OSM-induced differentiation of breast cancer cells is associated with increased TGF-β as well as EGF receptor levels suggesting that OSM could drive

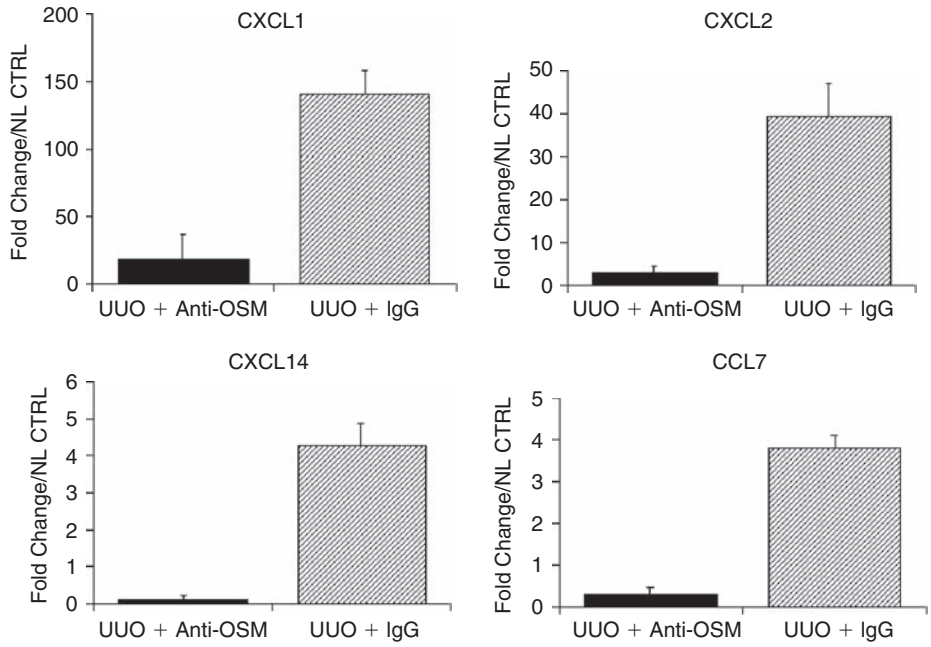

FIG. 8. Oncostatin M (OSM) antagonism reduces renal chemokine expression in murine renal fibrosis. Treatment of unilateral ureteral obstruction (UUO)-induced murine renal fibrosis with neutralizing OSM results in a significant reduction of renal chemokine mRNA expression. Graphics illustrate the mean relative chemokine mRNA expression compared with the contralateral non-ligated control kidney of each mouse.

the expression of other EMT-inducing factors (Douglas and others 1998).

To confirm that OSM/OSM-R system is associated with renal obstruction, we conducted a time-course analysis of OSM and OSM-R expression in UUO models, in both mouse and rat. The results clearly demonstrate a progressive increase of OSM and its receptor very early (within hours) following UUO. Protein localization revealed TECs and glomeruli have higher OSM and OSM-R levels following obstruction. Furthermore, up-regulation of the OSM/OSM-R system developed just shortly after UUO, and preceded the onset of any transdifferentiation as evident by absence of increase in EMT markers (α-SMA and collagen I) within the first 24 h following UUO. Indeed, the dynamic pattern of EMT markers is well documented by Liu (2004). Using obstructive nephropathy as a model, this group determined that α-SMA induction takes place in the period ranging from 1 day to 3 days, while E-cadherin levels reached the lowest level 7 days after UUO. There have been many reports that demonstrate an increase in EMT markers such as α-SMA and collagen I at least 3 days post-UUO (Yang and others 2002; Liu 2006; Qi and others 2006).

Nightingale and coworkers previously proposed that OSM is likely produced by inflammatory infiltrates into kidney interstitium. Indeed, there is a correlation between tubular atrophy, interstitial fibrosis, and the extent of interstitial infiltration (Papayianni 1996; Schena and others 1997). Infiltrating leukocytes produce proinflammatory and profibrotic cytokines that contribute to fibroblast proliferation, myofibroblast transdifferentiation, matrix production, and tubular atrophy. However, our studies clearly demonstrate OSM/OSM-R up-regulation preferentially in TECs and this up-regulation was not attributable to inflammatory infiltrates to the kidney. A progressive interstitial accumulation of T cells, macrophages, and lymphocytes in obstructed kidneys usually occurs at least 1 day following UUO (Vielhauer and others 2001; Sato and others 2003). Thus, it is possible that OSM could be produced by infiltrates at a later stage of UUO; however, early production of OSM (within the first 12 h post-UUO) is attributed to resident renal cells; namely, TECs.

OSM participates in growth regulation, differentiation, gene expression, and cell survival in a variety of cell types, and also contributes to inflammation and tissue remodeling processes (Tanaka and Miyajima 2003). Recently, OSM has been shown to play an important role in early polymorphonuclear cells (PMN) recruitment during wound inflammation (Goren and others 2006). Three major cell types are established as producers of OSM under different conditions *in vitro* and *in vivo*: activated T lymphocytes (Brown and others 1987), activated monocytes (Zarling and others 1986), and PMNs (Grenier and others 1999). In renal obstruction, PMNs represent the very first immune cells, infiltrating within the first 12–24 h into the injured kidney (Vielhauer and others 2001; Sato and others 2003). Thus, it is possible that the rapid increase in OSM produced by TECs and glomeruli might be connected, at least partially, to the early PMN recruitment. This is further explored using a microarray gene expression approach.

We first demonstrated that OSM is expressed very early (within hours) following kidney obstruction consistent with initial radioimmunoassay results and real-time PCR analysis of UUO versus sham-operated kidneys. Further molecular analysis of gene expression profiles revealed up-regulated gene expression of certain chemokines. Indeed, addition of recombinant OSM protein *in vitro* to kidney fibroblasts up-regulated CXCL14 and CCL7 whose expression was also up-regulated based on microarray analysis in

obstructed kidneys. However, our *in vivo* studies involving neutralization of OSM protein shortly before onset of UUO dramatically attenuated the mRNA expression of CXCL1, CXCL2, CXCL14, and CCL7 in obstructed kidneys. Based on studies with cultured cells, different cell types have the potential to generate various amounts of many chemokines; however, the pattern of chemokine expression *in vivo* can be much more selective (Kopydlowski and others 1999). Nevertheless, the effect of OSM neutralization immediately following UUO suggests that OSM likely secreted by resident renal cells is capable of modulating the expression of a number of chemokines that may facilitate additional leukocyte recruitment, local inflammation, and tubulointerstitial injury.

OSM promotes EMT in human TECs (Nightingale and others 2004). Biological activities of human OSM are mediated through binding to gp130 and either leukemia inhibitory factor receptor- or OSM-R to form OSM-signaling receptor complex I or II, respectively (Tanaka and Miyajima 2003). However, the murine OSM restrictively transduces signals through its specific receptor complex composed of gp130 and OSM-R-β, but not through the LIF receptor. We confirmed that as in human cells, OSM can promote the EMT phenomenon in rodent cells as well. Under the influence of OSM, rat renal TEC line, NRK52E, underwent transdifferentiation, as indicated by *de novo* expression of mesenchymal markers and morphologic changes.

Loss of epithelial cell adhesion is an early key event that precedes other alterations during EMT (Yang and Liu 2001). E-cadherin, an adhesion receptor found within adherens type junctions, plays a role in maintaining the polarity and structural integrity of renal epithelial cells. Consequently, loss of E-cadherin would destabilize the structural integrity of renal epithelium and weaken epithelial connections. The addition of antibodies to E-cadherin induces disaggregation of the MDCK kidney epithelial cell line and their reversal to fibroblast-like cells (Behrens and others 1985). In our study, the transfected TECs were further characterized by examining the stability of their cell–cell adhesion using impedance analysis. The presence of OSM caused "weakening" of junctional adhesions.

In conclusion, our results collectively offer for the first time a correlation between the levels of OSM and chronic tubulointerstitial fibrosis in human obstructive nephropathy. Similarly, urinary obstruction in murine models leads to early activation of the OSM/OSM-R system before tubulointerstitial fibrosis. This activation, likely attributed to resident renal cells but not inflammatory cell infiltrates, consequently modulate chemokine expression to attract further inflammatory cells. We also confirmed that similar to human TECs, OSM stimulates EMT in rodent TECs *in vitro*. Thus, we speculate that very early obstructive injury of the kidney induces elevated OSM/OSM-R expression, which plays a potent role in driving EMT, leading eventually to renal interstitial fibrosis.

Acknowledgments

Work was supported by the National Institutes of Health grant DK064233 and USDA 6250-51000-046. The authors would like to thank Dr. Sue Chunliu, Dr. Xiao R. Lan, Dr. Zhijie Li, Dr. Zhaoyong Hu, and Dr. Robert Collins for their generous support and technical assistance.

Author Disclosure Statement

No competing financial interests exist.

References

Behrens J, Birchmeier W, Goodman SL, Imhof BA. 1985. Dissociation of Madin-Darby canine kidney epithelial cells by the monoclonal antibody anti-arc-1: mechanistic aspects and identification of the antigen as a component related to uvomorulin. J Cell Biol 101(4):1307–1315.

Brown TJ, Lioubin MN, Marquardt H. 1987. Purification and characterization of cytostatic lymphokines produced by activated human T lymphocytes. Synergistic antiproliferative activity of transforming growth factor beta 1, interferon-gamma, and oncostatin M for human melanoma cells. J Immunol 139(9):2977–2983.

Dauthville S, Fischer E, Mougenot B, Delauche M, Ronco P, Rossert J. 1998. Identification of type I collagen-producing cells during interstitial fibrosis induced by unilateral ureteral obstruction. J Am Soc Nephrol 9:514A.

De Longh RU, Wederll E, Lovicu FJ, McAvoy JW. 2005. Transforming growth factor—induced epithelial-mesenchymal transition in the lens: a model for cataract formation. Cells Tissues Organs 179:43–55.

Douglas AM, Grant SL, Goss GA, Clouston DR, Sutherland RL, Begley CG. 1998. Oncostatin M induces the differentiation of breast cancer cells. Int J Cancer 75(1):64–73.

Fan JM, Ng YY, Hill PA, Nikolic-Paterson DJ, Mu W, Atkins RC, Lan HY. 1999. Transforming growth factor-beta regulates tubular epithelial-myofibroblast transdifferentiation in vitro. Kidney Int 56(4):1455–1467.

Feng L, Garcia GE, Yang Y, Xia Y, Gabbai FB, Peterson OW, Abraham JA, Blantz RC, Wilson CB. 2000. Heparin-binding EGF-like growth factor contributes to reduced glomerular filtration rate during glomerulonephritis in rats. J Clin Invest 105(3):341–350.

Fukuda K, Yoshitomi K, Yanagida T, Tokumoto M, Hirakata H. 2001. Quantification of TGF-beta1 mRNA along rat nephron in obstructive nephropathy. Am J Physiol Renal Physiol 281(3):F513–F521.

Gatsios P, Haubeck HD, Van de Leur E, Frisch W, Apte SS, Greiling H, Heinrich PC, Graeve L. 1996. Oncostatin M differentially regulates tissue inhibitors of metalloproteinases TIMP-1 and TIMP-3 gene expression in human synovial lining cells. Eur J Biochem 241(1):56–63.

Goren I, Kämpfer H, Müller E, Schiefelbein D, Pfeilschifter J, Frank S. 2006. Oncostatin M expression is functionally connected to neutrophils in the early inflammatory phase of skin repair: implications for normal and diabetes-impaired wounds. J Invest Dermatol 126(3):628–637.

Grenier A, Dehoux M, Boutten A, Arce-Vicioso M, Durand G, Gougerot-Pocidalo MA, Chollet-Martin S. 1999. Oncostatin M production and regulation by human polymorphonuclear neutrophils. Blood 93(4):1413–1421.

Hasegawa M, Sato S, Ihn H, Takehara K. 1999. Enhanced production of interleukin-6 (IL-6), oncostatin M and soluble IL-6 receptor by cultured peripheral blood mononuclear cells from patients with systemic sclerosis. Rheumatology (Oxford) 38(7):612–617.

Hay ED, Zuk A. 1995. Transformations between epithelium and mesenchyme: normal, pathological, and experimentally induced. Am J Kidney Dis 26(4):678–690.

Healy E, Leonard M, Madrigal-Estebas L, O'Farrelly C, Watson AJ, Ryan MP. 1999. Factors produced by activated leukocytes alter renal epithelial cell differentiation. Kidney Int 56(4):1266–1269.

Jinde K, Nikolic-Paterson DJ, Huang XR, Sakai H, Kurokawa K, Atkins RC, Lan HY. 2001. Tubular phenotypic change in

progressive tubulointerstitial fibrosis in human glomerulonephritis. Am J Kidney Dis 38(4):761–769.
Kopydlowski KM, Salkowski CA, Cody MJ, van Rooijen N, Major J, Hamilton TA, Vogel SN. 1999. Regulation of macrophage chemokine expression by lipopolysaccharide *in vitro* and *in vivo*. J Immunol 163(3):1537–1544.
Lan HY. 2003. Tubular epithelial-myofibroblast transdifferentiation mechanisms in proximal tubule cells. Curr Opin Nephrol Hypertens 12(1):25–29.
Lan HY, Mu W, Tomita N, Huang XR, Li JH, Zhu HJ, Morishita R, Johnson RJ. 2003. Inhibition of renal fibrosis by gene transfer of inducible Smad7 using ultrasound-microbubble system in rat UUO model. J Am Soc Nephrol 14(6):1535–1548.
Liu Y. 2004. Epithelial to mesenchymal transition in renal fibrogenesis: pathologic significance, molecular mechanism, and therapeutic intervention. J Am Soc Nephrol 15(1):1–12.
Liu Y. 2006. Renal fibrosis: new insights into the pathogenesis and therapeutics. Kidney Int 69(2):213–217.
Lo CM, Keese CR, Giaever I. 1993. Monitoring motion of confluent cells in tissue culture. Exp Cell Res 204(1):102–109.
Luyckx VA, Cairo LV, Compston CA, Phan WL, Mueller TF. 2009. Oncostatin M pathway plays a major role in the renal acute phase response. Am J Physiol Renal Physiol 296(4):F875–F883.
Malaval L, Liu F, Vernallis AB, Aubin JE. 2005. GP130/OSMR is the only LIF/IL-6 family receptor complex to promote osteoblast differentiation of calvaria progenitors. J Cell Physiol 204(2):585–593.
Malik N, Haugen HS, Modrell B, Shoyab M, Clegg CH. 1995. Developmental abnormalities in mice transgenic for bovine oncostatin M. Mol Cell Biol 15(5):2349–2358.
Manotham K, Tanaka T, Matsumoto M, Ohse T, Inagi R, Miyata T, Kurokawa K, Fujita T, Ingelfinger JR, Nangaku M. 2004. Transdifferentiation of cultured tubular cells induced by hypoxia. Kidney Int 65(3):871–880.
Morikawa Y, Tamura S, Minehata K, Donovan PJ, Miyajima A, Senba E. 2004. Essential function of oncostatin m in nociceptive neurons of dorsal root ganglia. J Neurosci 24(8):1941–1947.
Nadasdy T, Laszik Z, Blick KE, Johnson DL, Silva FG. 1994. Tubular atrophy in the end-stage kidney: a lectin and immunohistochemical study. Hum Pathol 25(1):22–28.
Ng YY, Fan JM, Mu W, Nikolic-Paterson DJ, Yang WC, Huang TP, Atkins RC, Lan HY. 1999. Glomerular epithelial-myofibroblast transdifferentiation in the evolution of glomerular crescent formation. Nephrol Dial Transplant 14(12):2860–2872.
Ng YY, Huang TP, Yang WC, Chen ZP, Yang AH, Mu W, Nikolic-Paterson DJ, Atkins RC, Lan HY. 1998. Tubular epithelial-myofibroblast transdifferentiation in progressive tubulointerstitial fibrosis in 5/6 nephrectomized rats. Kidney Int 54(3): 864–876.
Nightingale J, Patel S, Suzuki N, Buxton R, Takagi KI, Suzuki J, Sumi Y, Imaizumi A, Mason RM, Zhang Z. 2004. Oncostatin M, a cytokine released by activated mononuclear cells, induces epithelial cell-myofibroblast transdifferentiation via Jak/Stat pathway activation. J Am Soc Nephrol 15(1):21–32.
Okada H, Danoff TM, Kalluri R, Neilson EG. 1997. Early role of Fsp1 in epithelial-mesenchymal transformation. Am J Physiol 273(4 Pt 2):F563–F574.
Okaya A, Kitanaka J, Kitanaka N, Satake M, Kim Y, Terada K, Sugiyama T, Takemura M, Fujimoto J, Terada N, Miyajima A, Tsujimura T. 2005. Oncostatin M inhibits proliferation of rat oval cells, OC15-5, inducing differentiation into hepatocytes. Am J Pathol 166(3):709–719.
Papayianni A. 1996. Cytokines, growth factors, and other inflammatory mediators in glomerulonephritis. Ren Fail 18(5):725–740.
Qi W, Chen X, Poronnik P, Pollock CA. 2006. The renal cortical fibroblast in renal tubulointerstitial fibrosis. Int J Biochem Cell Biol 38(1):1–5.
Rastaldi MP, Ferrario F, Giardino L, Dell'Antonio G, Grillo C, Grillo P, Strutz F, Müller GA, Colasanti G, D'Amico G. 2002. Epithelial-mesenchymal transition of tubular epithelial cells in human renal biopsies. Kidney Int 62(1):137–146.
Sato M, Yasuteru M, Saika S, Roberts AB, Ooshima A. 2003. Targeted disruption of TGF-1/Smad3 signaling protects against renal tubulointerstitial fibrosis induced by unilateral ureteral obstruction. J Clin Inv 112:1486–1494.
Scaffidi AK, Mutsaers SE, Moodley YP, McAnulty RJ, Laurent GJ, Thompson PJ, Knight DA. 2002. Oncostatin M stimulates proliferation, induces collagen production and inhibits apoptosis of human lung fibroblasts. Br J Pharmacol 136(5):793–801.
Schena FP, Gesualdo L, Grandaliano G, Montinaro V. 1997. Progression of renal damage in human glomerulonephritides: is there sleight of hand in winning the game? Kidney Int 52(6):1439–1457.
Stahl PJ, Felsen D. 2001. Transforming growth factor-beta, basement membrane, and epithelial-mesenchymal transdifferentiation: implications for fibrosis in kidney disease. Am J Pathol 159(4):1187–1192.
Strutz F, Müller GA. 2000. Transdifferentiation comes of age. Nephrol Dial Transplant 15(11):1729–1731.
Tanaka M, Miyajima A. 2003. Oncostatin M, a multifunctional cytokine. Rev Physiol Biochem Pharmacol 149:39–52.
Thiery JP, Sleeman JP. 2006. Complex networks orchestrate epithelial-mesenchymal transitions. Nat Rev Mol Cell Biol 7(2): 131–142.
Vielhauer V, Anders HJ, Mack M, Cihak J, Strutz F, Stangassinger M, Luckow B, Gröne HJ, Schlöndorff D. 2001. Obstructive nephropathy in the mouse: progressive fibrosis correlates with tubulointerstitial chemokine expression and accumulation of CC chemokine receptor 2- and 5-positive leukocytes. J Am Soc Nephrol 12(6):1173–1187.
Yang J, Dai C, Liu Y. 2002. Hepatocyte growth factor gene therapy and angiotensin II blockade synergistically attenuate renal interstitial fibrosis in mice. J Am Soc Nephrol 13(10):2464–2477.
Yang J, Liu Y. 2001. Dissection of key events in tubular epithelial to myofibroblast transition and its implications in renal interstitial fibrosis. Am J Pathol 159(4):1465–1475.
Zarling JM, Shoyab M, Marquardt H, Hanson MB, Lioubin MN, Todaro GJ. 1986. Oncostatin M: a growth regulator produced by differentiated histiocytic lymphoma cells. Proc Natl Acad Sci USA 83(24):9739–9743.
Zeisberg M, Strutz F, Müller GA, Kalluri R. 1999. Epithelial-mesenchymal transdifferentiation (EMT) in renal fibrogenesis: disruption of type IV collagen with soluble NCα1 domains induces EMT. Kidney Blood Pres Res 22:255–256.

Address correspondence to:
Dr. Wafa Elbjeirami
King Hussein Cancer Center
Queen Rania Al Abdullah Street
P.O. Box 1269 AL-Jubeiha
Amman 11941
Jordan

E-mail: wbjeirami@khcc.jo

Received 22 October 2009/Accepted 18 December 2009